Biochemical and Biophysical Research Communications 532 (2020) 336–340

Contents lists available at ScienceDirect

Biochemical and Biophysical Research Communications

journal homepage: www.elsevier.com/locate/ybbrc

Loss of GM130 does not impair oocyte meiosis and embryo development in mice

Yonghui Jiang [a, b], Yue Liu [a, b], Feng Han [c], Jingjing Zhou [c], Xinze Zhang [a, b], Junting Xu [a, b], Zhiheng Yu [a, b], Shigang Zhao [a, b], Fei Gao [c, *], Han Zhao [a, b, **]

[a] Center for Reproductive Medicine, Cheeloo College of Medicine, Shandong University, Jinan, 250001, China
[b] Key Laboratory of Reproductive Endocrinology of Ministry of Education, Shandong University, Jinan, Shandong, 250012, China
[c] State Key Laboratory of Reproductive Biology, Institute of Zoology, Chinese Academy of Science, Beijing, 100101, China

ARTICLE INFO

Article history:
Received 14 August 2020
Accepted 19 August 2020
Available online 30 August 2020

Keywords:
GM130
Oocytes
Meiosis
In vivo

ABSTRACT

Golgi matrix protein 130 (GM130), encoded by *GOLGA2*, is the classical marker of the Golgi apparatus. It plays important roles in various mitotic events, such as interacting with importin-alpha and liberating spindle assembly factor TPX2 to regulate mitotic spindle formation. A previous study showed that *in vitro* knockdown of GM130 could regulate the meiotic spindle pole assembly. In the current study, we found that knockout (KO) mice progressively died, had a small body size and were completely infertile. Furthermore, we constructed an oocyte-specific *GM130* knockout mouse model (*GM130*-ooKO) driven by Gdf9-Cre. Through breeding assays, we found that the *GM130*-ooKO mice showed similar fecundity as control mice. During superovulation assays, the KO and *GM130*-ooKO mice had comparable numbers of ovulated eggs, oocyte maturation rates and normal polar bodies, similar to the control groups. Thus, this study indicated that deletion of *GM130* might have a limited impact on the maturation and morphology of oocytes. This might due to more than one golgin sharing the same function, with others compensating for the loss of GM130.

1. Introduction

The Golgi apparatus is a highly ordered polar organelle formed by several flattened vesicles stacked together, often distributed between the endoplasmic reticulum and cell membrane. Its main function is to process, modify, classify and package the proteins synthesized by the endoplasmic reticulum, and then deliver them to specific parts of the cell or secrete them outside the cell. The Golgi apparatus has highly dynamic changes during the cell cycle process, and its structural and functional alterations affect various cell biological events such as intracellular material transport, signal transduction, and cell proliferation and apoptosis in different ways [1,2]. The Golgi apparatus is distributed in different patterns at different stages of oocyte maturation; for example, they are scattered around the nucleolus in bovine GV oocytes, congregate in the cortical region during germinal vesicle breakdown (GVBD), and are uniformly distributed in the cytoplasm at the MII stage [3]. It has been shown that the Golgi apparatus is quickly destroyed when oocytes are treated with Brefeldin A (BFA, an inhibitor of Golgi-based membrane fusion). The rate of oocyte maturation decreased along with abnormal polar body formation, which means that a normal Golgi apparatus is necessary for *in vitro* oocyte maturation [4].

Golgi matrix protein 130 (GM130), encoded by the *Golga2* gene, is the classical marker of the Golgi apparatus. GM130 is highly conserved and interacts with P115, giantin, GRASP65, and Rab GTPases to maintain the Golgi structure, control glycosylation, and participate in membrane-vesicle transport [5]. Recently, many *in vitro* experiments have revealed that GM130 plays important roles in cell cycle progression, maintenance of cell polarity, cell migration, and autophagy [5]. Chang et al. [6] found that GM130-deficient tumour cell lines had enhanced proliferation and increased autophagy levels. Joachim et al. [7] revealed that GM130 promotes the formation of autophagosomes when interacting with WAC and negatively regulates the autophagy process when interacting with GABARAP. Wei et al. [8] confirmed that GM130 regulates cell mitosis by promoting the activation of spindle assembly

* Corresponding author.
** Corresponding author. Center for Reproductive Medicine, Cheeloo College of Medicine, Shandong University, Jinan, 250001, China.
E-mail addresses: gaof@ioz.ac.cn (F. Gao), hanzh80@yahoo.com (H. Zhao).

https://doi.org/10.1016/j.bbrc.2020.08.055
0006-291X/

factor TPX2. Using an *in vitro* knockdown assay, Sun's group reported that GM130 can regulate microtubule assembly through collaboration with the MAPK signalling pathway and influence mouse oocyte spindle assembly, migration and asymmetric division. Very few studies have focused on GM130 in oocyte maturation and early embryo development. To date, there is still a lack of evidence about the role of GM130 during meiosis and early embryonic development *in vivo*. Therefore, we constructed whole knockout as well as oocyte-specific knockout mouse models and tried to delineate the role of GM130 during oocyte meiosis.

2. Materials and methods

2.1. Animals

All animal experiments were conducted in accordance with the Animal Research Committee guidelines of Shandong University. Mice were housed in an environment with a stable temperature (20–22 °C), 12/12-h light/dark cycle, 50–70% humidity, and provided with adequate food and water at periodic intervals. *GM130* $^{flox/flox}$ mice were kindly gifted by Dr. Shilai Bao (Institute of Genetics and Developmental Biology, Chinese Academy of Sciences, Beijing, China). *GM130* $^{flox/flox}$ *Gdf9-Cre* female mice were created by crossing *GM130* $^{flox/+}$ *Gdf9-Cre* male mice with *GM130* $^{flox/+}$ females. All the mice in the assays had a mixed background. Genotyping was identified via PCR using DNA isolated from the tail. The primers were as follows: GM130 flox allele forward primer, 5′-TTGTTCAACAGTGGAGCCCT-3′; reverse primer, 5′-TGAAGGCATTTCAACAGGCG-3′; GM130−allele forward primer, 5′-GCCTTTCATTCCTAGCATTTGG-3′; reverse primer, 5′- GGGCTCACACCTGCAACCT-3′, GDF9-Cre forward primer, 5′- AAGAACCTGATGGACATGTTCAG-3′; reverse primer, 5′-CTGATCCTGGCAATTTCGG-3′.

2.2. Breeding and superovulation assay

For breeding assays, male and female mice were mated at 1:2, and the number of pups per litter was counted. For superovulation assays, female mice (21–23 days) were injected intraperitoneally with 5 IU pregnant mare serum gonadotropin (PMSG) and 44 h later with 5 IU hCG (Ningbo Sansheng Pharmaceutical Co., Ltd., China). After 16 h, cumulus-oocyte-complexes (COCs) were obtained from the enlarged part of the oviduct, and the number of oocytes were counted after the removal of granulosa cells. The first polar body discharge was counted and photographed using a Nikon SMZ1500 stereomicroscope.

2.3. Immunofluorescence

Oocytes were fixed in 4% paraformaldehyde (PFA) in PBS and incubated with 0.2% Triton X-100 in PBS for 30 min. Afterwards, the zona pellucida was removed with 0.5% Pronase E (P8811, Sigma-Aldrich). Then, the cells were blocked with 1% BSA in washing buffer (PBST: PBS with 0.1% Triton X-100). After that, oocytes were incubated with GM130 antibodies (1:50 dilution; #610823, BD Biosciences) buffered in the blocking solution. After three washes, oocytes were mounted using VECTASHIELD medium with DAPI (#H-1200, Vector Laboratories). Immunolabelled oocytes were imaged by confocal microscopy (Dragonfly, Andor Technology). Images were then prepared using ImageJ Software (NIH, v. 1.6.0–65) or Bitplane Imaris (v8.1) software.

2.4. Haematoxylin and eosin (H&E) staining

Immediately after euthanasia, ovaries (appendages) of at least three mice per genotype were dissected, fixed with Bouin's solution (HT10132, Sigma-Aldrich) for up to 24 h, and stored in 70% ethanol until dehydrated. Then, the tissues were paraffin-embedded, and 5-μm sections were prepared (RM2235, Leica) and mounted on glass slides (#80312, CITOTEST). After de-paraffinization, the tissues on the slides were stained with haematoxylin and eosin. The slides were photographed using an inverted microscope (BX52, Olympus).

2.5. Western blotting

To prepare protein extracts, ovaries were collected from PD21 mice, and total protein was extracted using a commercial Minute™ Total Protein Extraction Kit (SD-001, Invent) plus protease inhibitors (P1005, Beyotime). The supernatants were used for Western blotting. Equal amounts of protein were electrophoresed on 8% Tris-Glycine gels, and the bands were transferred to polyvinylidene fluoride membranes (IPVH00010, Millipore). The primary antibodies for immunoblotting included GM130 (1:5000 dilution, 11308-1-AP, Proteintech Group) and β-actin (1:5000 dilution; A5441, Sigma-Aldrich). Immunoreactive bands were detected using Immobilon Western HRP Substrate Peroxide Solution (WBKLS0100, Millipore) and analysed with a Bio-Rad ChemiDoc MP Imaging System and Image Lab Software (Bio-Rad).

2.6. Statistical analysis

The results are presented as the mean ± SD; each experiment was repeated at least 3 times. A two-tailed unpaired Student's t-test was used for comparisons between groups. A P-value < 0.05 was considered significant.

3. Results

3.1. *GM130*$^{-/-}$ females showed growth retardation and infertility

To investigate the role of GM130 in reproduction, we employed *GM130* knockout mice (*GM130*$^{-/-}$) as our study objects (Fig. 1. A and B). GM130 was completely undetectable in the ovarian tissues of *GM130*$^{-/-}$ mice at postnatal day 21 (PD21) (Fig. 1. C). Consistent with previously studies [9], *GM130*$^{-/-}$ females were viable, and the birth rate was consistent with the Mendelian ratio. However, GM130 deficiency resulted in growth restriction. The body weight of *GM130*$^{-/-}$ females was about half of that of control mice at PD21 (Fig. 1. D). The KO mice progressively died since PD30. The maximum lifespan of *GM130*$^{-/-}$ females was approximately 80 days, and the remaining *GM130*$^{-/-}$ females were completely infertile (Fig. 1. E).

3.2. *GM130*$^{-/-}$ female mice could ovulate normally at PD21

We further tested the knockout efficiency of GM130 in oocytes by immunofluorescence. The *GM130*$^{-/-}$ mouse oocytes showed a completely undetectable GM130 signal (Fig. 2. A). GM130 was distributed widely in the cytoplasm in control MII oocytes. We then performed superovulation assays on *GM130*$^{-/-}$ female mice. Although the *GM130*$^{-/-}$ mice were small, the oocyte numbers were comparable (Fig. 2. B). To further evaluate the quality of the oocytes, the MII oocyte morphology and first polar body (PB1) extrusion rate were compared. The results showed that PB1 extrusion rates between *GM130*$^{-/-}$ and control mice were similar and the MII oocyte morphology was robustly normal (Fig. 2. C and D). The inserted images represent MII oocytes with no obvious morphological abnormalities, and the black arrows point to PB1 (Fig. 2. D). After superovulation, the histology of KO ovaries was grossly normal

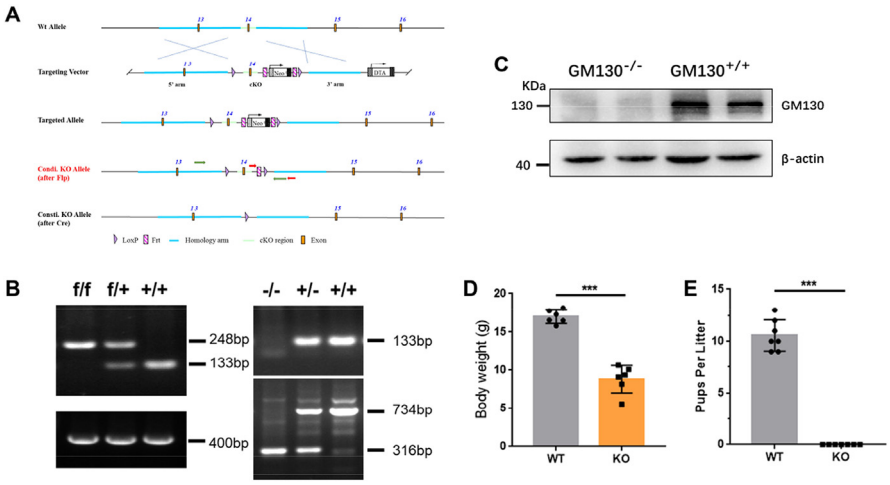

Fig. 1. Loss of GM130 in female mice results in growth restriction and infertility. (A) Scheme for generating GM130 KO mice; (B) Knockout mouse genotyping by PCR; (C) Western blotting for GM130 in ovaries; (D) Body weight at postnatal day 21; (E) Breeding assays in different mouse genotypes, n = 6 each group. *** indicates $p < 0.001$.

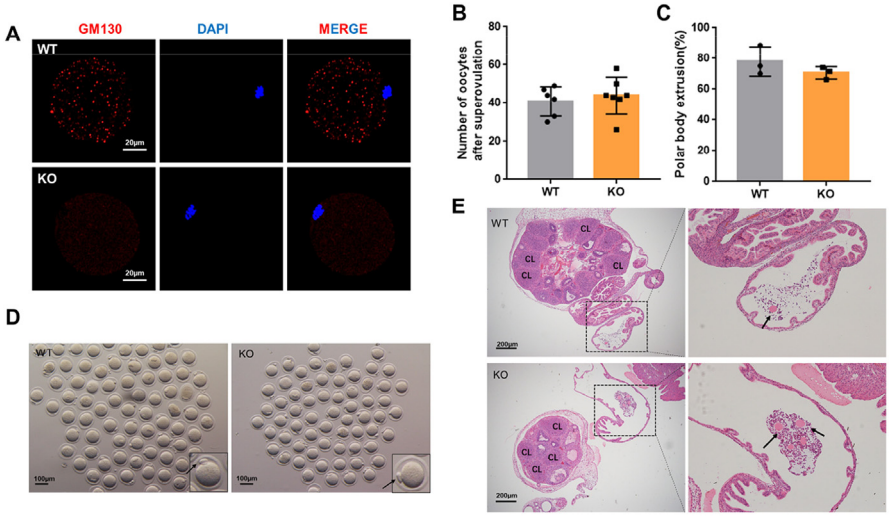

Fig. 2. Female mice that lost GM130 ovulated normally at PD21. (A) Oocyte immunofluorescent staining for GM130, scale bar = 20 μm; (B) Number of oocytes obtained after superovulation, n = 6 vs 7; (C) Polar body extrusion rate, three independent experiments; (D) Morphology of MII oocytes under DIC, where black arrows indicate polar bodies, scale bar = 100 μm; (E) Haematoxylin and eosin (H&E) staining of the ovary and oviduct after superovulation, where black arrows indicate COC, CL = corpus luteum, scale bar = 200 μm.

compared with the controls. Both groups of mice had an obvious corpus luteum, consistent with post-ovulatory morphology (Fig. 2. E). In addition, cumulus-oocyte-complexes (COCs) could be seen in the ampulla of the uterine tubes (Fig. 2. E, black arrows), indicating that female mice without GM130 could ovulate.

3.3. *GM130 $^{f/f}$ Gdf9-Cre females were fertile*

The KO mice showed growth retardation, and to precisely explore the role of GM130 in oocytes, we generated oocyte-specific GM130 knockout mice (*GM130 $^{f/f}$ Gdf9-Cre*; *GM130* oo-KO). The immunofluorescence results showed that GM130 expression was indeed absent in *GM130*-ooKO mice (Fig. 3. A). In addition, *GM130*-ooKO mice showed no significant abnormalities in growth and development, and the body weight was comparable with wildtypes at PD21 and PD180 (Fig. 3. B). The breeding assay showed that *GM130* oo-KO females were fertile, and there was no significant difference in the number of pups per litter over 6 months (Fig. 3. C). After superovulation, there were no obvious abnormalities in the oocyte acquisition and polar body extrusion rate in *GM130* oo-KO females (Fig. 3 D-F). The HE staining of ovaries after superovulation also showed no significant difference (Fig. 3. G), which was consistent with the comparable corpus luteum.

4. Discussion

In this study, we found that *GM130* KO mice had growth retardation, progressive death and complete infertility. The oocyte-specific *GM130* KO mice developed normally with normal fertility. These two lines of mice could ovulate normally with roughly normal eggs. The results indicated that deletion of *GM130* might have limited impacts on the maturation and morphology of oocytes, and this may be compensated for by other golgins or granulosa cells.

Previously, Liu et al. found that whole-body knockout of *GM130* led to growth retardation and severe ataxia in mice, with an approximately 80% death rate at 35 days post-birth on a C57BL/6 background [9]. This is in line with our breeding assays. Park et al.

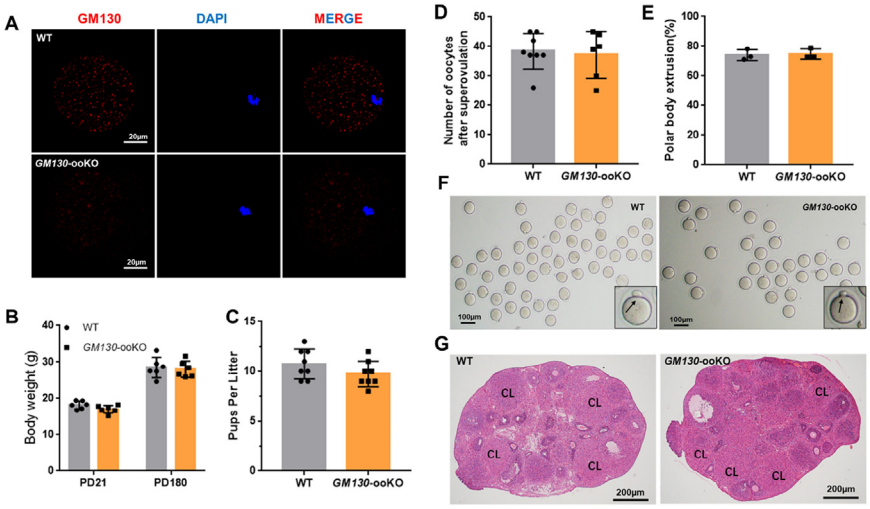

Fig. 3. Female mice with oocyte-specific knockout of GM130 grew normally and were fertile. (A) Oocyte immunofluorescent staining for GM130, scale bar = 20 μm; (B) Body weight at PD21, n = 6 in each group; (C) Pups per litter of indicated mice; (D) Number of oocytes obtained after superovulation, n = 8 vs 6; (E) Polar body extrusion rate, three independent experiments; (F) Morphology of MII oocytes under DIC, where black arrows indicate polar bodies, scale bar = 100 μm; (G) Haematoxylin and eosin (H&E) staining of the ovary after superovulation, CL = corpus luteum, scale bar = 200 μm.

found that Golgi destruction in *GM130*-deficient mice resulted in a dramatic increase in autophagy levels and fibrotic symptoms in the lung and liver [11]. For reproduction, *GM130*-deficient male mice are completely sterile, with sperm lacking acrosomes, a complete disappearance of the middle mitochondrial sheath, and a rounded sperm head. That is, they exhibit round-headed spermatozoa. Male germ cell-specific knockouts of *GM130* resulted in a phenotype similar to that of whole knockout male mice, but a Sertoli cell-specific knockout of *GM130* did not affect germ cell development [12]. Sun's group revealed that GM130 can regulate microtubule assembly through collaboration with the MAPK signalling pathway in mouse oocytes [10]. However, similar alterations were not observed in our study. This has led to the suggestion that the loss of GM130 might be compensated for by other golgins [13,14].

The Golgi apparatus is a trafficking hub. Proteins from the endoplasmic reticulum (ER) can enter the *trans*-Golgi network (TGN) via the cisternae, from where they are transported to the endosomes, lysosomes and plasma membrane [15,16]. Crucially, the Golgi must maintain the molecular properties of its stacks while remaining flexible to exert its normal functions. The integrity of the Golgi apparatus consists of a number of golgins with large coiled-coil proteins on the cytoplasmic surface [17]. Golgins include GM130, p115, and GMAP-210 on the *cis*-Golgi, golgin-97, golgin-245, GCC88, and GCC185 on the *trans*-Golgi, and TMF, CASP, golgin-84, and giantin on the Golgi rims. In various *in vivo* studies, only the loss of p115 (an interaction partner of GM130) resulted in embryonic lethality, and the vast majority of ablation of individual golgins caused milder defects in certain cell types [18–22]. For example, GRASP65 (another interaction partner of GM130) KO mice were healthy and fertile with no apparent defects in tissue, cellular or subcellular organization [23]. More interestingly, there is a study reporting that female $TMF^{-/-}$ mice developed normally and were fertile, while male $TMF^{-/-}$ mice were sterile and their sperm suffered from severe key malformations [24]. The above indicates that golgins such as GM130 and TMF may act differently in females and males.

Knock down of golgin expression *in vitro* resulted in Golgi fragmentation and dispersion of Golgi marker proteins throughout the cytoplasm [25–29]. Knock down of GM130 by specific morpholino microinjection caused abnormal spindle formation and decreased first polar body extrusion [10]. However, in this study, oocyte-specific knockout of GM130 did not exhibit the same phenotype as previous studies. This might due to more than one golgin sharing the same function, indicating that others may compensate for the loss of GM130. Two recent back-to-back publications have revealed the molecular mechanisms of the genetic compensation effect. Specifically, those genetic mutations without a phenotype can produce non-sense mRNAs and non-sense mRNA mediated decay (NMD). The NMD can interact directly with the COMPASS (complex of proteins associated with Set1) complex to activate homologous gene expression for functional compensation [30,31]. We suspected that deletion of GM130 *in vivo* might also have a compensatory mechanism, and this compensatory mechanism might have cell specificity (oocyte or sperm). However, we still do not know what gene compensates for the GM130 mutation or how the compensatory gene is recognized. In the future, much work still needs to be done to answer these questions.

In conclusion, our results showed that loss of GM130 might not impair oocyte meiosis and embryonic development, and the infertility of knockout females may be due to growth retardation.

Declaration of competing interest

The authors declare that they have no competing interests.

Acknowledgements

We thank Professor Hengyu Fan for kindly gifting us *Gdf9-Cre* mice. This study was funded by the National Natural Science Foundation of China (31871509), Key Research and Development Program of Shandong Province (2019GSF108274), the National Natural Science Foundation of Shandong Province (JQ201816), the innovative research team of high-level local universities in Shanghai (SSMU-ZLCX20180401), the Young Scholars Program and The Fundamental Research Funds of Shandong University.

References

[1] I. Ayala, F. Mascanzoni, A. Colanzi, The Golgi ribbon: mechanisms of maintenance and disassembly during the cell cycle, Biochem. Soc. Trans. 48 (2020) 245–256.
[2] S. Huang, Y. Wang, Golgi structure formation, function, and post-translational modifications in mammalian cells, F1000Res 6 (2017) 2050.

[3] C. Payne, G. Schatten, Golgi dynamics during meiosis are distinct from mitosis and are coupled to endoplasmic reticulum dynamics until fertilization, Dev. Biol. 264 (2003) 50–63.
[4] S.E. Racedo, V.Y. Rawe, H. Niemann, Dynamic changes of the Golgi apparatus during bovine in vitro oocyte maturation, Reproduction 143 (2012) 439–447.
[5] N. Nakamura, Emerging new roles of GM130, a cis-Golgi matrix protein, in higher order cell functions, J. Pharmacol. Sci. 112 (2010) 255–264.
[6] S.H. Chang, S.H. Hong, H.L. Jiang, A. Minai-Tehrani, K.N. Yu, et al., GOLGA2/GM130, cis-Golgi matrix protein, is a novel target of anticancer gene therapy, Mol. Ther. 20 (2012) 2052–2063.
[7] J. Joachim, H.B. Jefferies, M. Razi, D. Frith, A.P. Snijders, et al., Activation of ULK kinase and autophagy by GABARAP trafficking from the centrosome is regulated by WAC and GM130, Mol. Cell 60 (2015) 899–913.
[8] J.H. Wei, Z.C. Zhang, R.M. Wynn, J. Seemann, GM130 regulates golgi-derived spindle assembly by activating TPX2 and capturing microtubules, Cell 162 (2015) 287–299.
[9] C. Liu, M. Mei, Q. Li, P. Roboti, Q. Pang, et al., Loss of the golgin GM130 causes Golgi disruption, Purkinje neuron loss, and ataxia in mice, Proc. Natl. Acad. Sci. U. S. A. 114 (2017) 346–351.
[10] C.H. Zhang, Z.B. Wang, S. Quan, X. Huang, J.S. Tong, et al., GM130, a cis-Golgi protein, regulates meiotic spindle assembly and asymmetric division in mouse oocyte, Cell Cycle 10 (2011) 1861–1870.
[11] S. Park, S. Kim, M.J. Kim, Y. Hong, A.Y. Lee, et al., GOLGA2 loss causes fibrosis with autophagy in the mouse lung and liver, Biochem. Biophys. Res. Commun. 495 (2018) 594–600.
[12] F. Han, C. Liu, L. Zhang, M. Chen, Y. Zhou, et al., Globozoospermia and lack of acrosome formation in GM130-deficient mice, Cell Death Dis. 8 (2017), e2532.
[13] A.K. Gillingham, S. Munro, Finding the golgi: golgin coiled-coil proteins show the way, Trends Cell Biol. 26 (2016) 399–408.
[14] N. Muschalik, S. Munro, Golgins, Curr. Biol. 28 (2018) R374–R376.
[15] E. Papanikou, B.S. Glick, Golgi compartmentation and identity, Curr. Opin. Cell Biol. 29 (2014) 74–81.
[16] B.S. Glick, A. Luini, Models for Golgi traffic: a critical assessment, Cold Spring Harb Perspect Biol 3 (2011) a005215.
[17] K. Nozawa, M.J. Fritzler, E.K. Chan, Unique and shared features of Golgi complex autoantigens, Autoimmun. Rev. 4 (2005) 35–41.
[18] S. Kim, A. Hill, M.L. Warman, P. Smits, Golgi disruption and early embryonic lethality in mice lacking USO1, PLoS ONE 7 (2012), e50530.
[19] Y. Elkis, S. Bel, T. Lerer-Goldstein, A. Nyska, D.M. Creasy, S. Shpungin, U. Nir, Testosterone deficiency accompanied by testicular and epididymal abnormalities in TMF(-/-) mice, Mol. Cell. Endocrinol. 365 (2013) 52–63.
[20] W. Zhou, J. Chang, X. Wang, M.G. Savelieff, Y. Zhao, S. Ke, B. Ye, GM130 is required for compartmental organization of dendritic golgi outposts, Curr. Biol. 24 (2014) 1227–1233.
[21] K. Katayama, T. Sasaki, S. Goto, K. Ogasawara, H. Maru, K. Suzuki, H. Suzuki, Insertional mutation in the Golgb1 gene is associated with osteochondrodysplasia and systemic edema in the OCD rat, Bone 49 (2011) 1027–1036.
[22] P. Smits, A.D. Bolton, V. Funari, M. Hong, E.D. Boyden, L. Lu, D.K. Manning, N.D. Dwyer, J.L. Moran, M. Prysak, B. Merriman, S.F. Nelson, L. Bonafé, A. Superti-Furga, S. Ikegawa, D. Krakow, D.H. Cohn, T. Kirchhausen, M.L. Warman, D.R. Beier, Lethal skeletal dysplasia in mice and humans lacking the golgin GMAP-210, N. Engl. J. Med. 362 (2010) 206–216.
[23] T. Veenendaal, T. Jarvela, A.G. Grieve, J.H. van Es, A.D. Linstedt, C. Rabouille, GRASP65 controls the cis Golgi integrity in vivo, Biol Open 3 (2014) 431–443.
[24] T. Lerer-Goldshtein, S. Bel, S. Shpungin, E. Pery, B. Motro, R.S. Goldstein, S.I. Bar-Sheshet, H. Breitbart, U. Nir, TMF/ARA160: a key regulator of sperm development, Dev. Biol. 348 (2010) 12–21.
[25] R.M. Ríos, A. Sanchís, A.M. Tassin, C. Fedriani, M. Bornens, GMAP-210 recruits gamma-tubulin complexes to cis-Golgi membranes and is required for Golgi ribbon formation, Cell 118 (2004) 323–335.
[26] M. Sohda, Y. Misumi, S. Yoshimura, N. Nakamura, T. Fusano, S. Sakisaka, S. Ogata, J. Fujimoto, N. Kiyokawa, Y. Ikehara, Depletion of vesicle-tethering factor p115 causes mini-stacked Golgi fragments with delayed protein transport, Biochem. Biophys. Res. Commun. 338 (2005) 1268–1274.
[27] M.A. Puthenveedu, C. Bachert, S. Puri, F. Lanni, A.D. Linstedt, GM130 and GRASP65-dependent lateral cisternal fusion allows uniform Golgi-enzyme distribution, Nat. Cell Biol. 8 (2006) 238–248.
[28] Y. Fridmann-Sirkis, S. Siniossoglou, H.R. Pelham, TMF is a golgin that binds Rab6 and influences Golgi morphology, BMC Cell Biol. 5 (2004) 18.
[29] T.N. Feinstein, A.D. Linstedt, GRASP55 regulates Golgi ribbon formation, Mol. Biol. Cell 19 (2008) 2696–2707.
[30] Z. Ma, P. Zhu, H. Shi, L. Guo, Q. Zhang, Y. Chen, S. Chen, Z. Zhang, J. Peng, J. Chen, PTC-bearing mRNA elicits a genetic compensation response via Upf3a and COMPASS components, Nature 568 (2019) 259–263.
[31] M.A. El-Brolosy, Z. Kontarakis, A. Rossi, C. Kuenne, S. Günther, N. Fukuda, K. Kikhi, G. Boezio, C.M. Takacs, S.L. Lai, R. Fukuda, C. Gerri, A.J. Giraldez, D. Stainier, Genetic compensation triggered by mutant mRNA degradation, Nature 568 (2019) 193–197.